ISSN 1946-7664. MCFNS 2012
Vol. 4, Issue 1, pp. 2–15
Mathematical and Computational Forestry & Natural-Resource Sciences

AVAILABLE ONLINE AT HTTP://MCFNS.COM

Submitted: Aug. 21, 2011
Accepted: Oct. 27, 2011
Published: Feb. 28, 2012
Last Correction: Feb. 28, 2012

TREE SHAPE AND BRANCH STRUCTURE: MATHEMATICAL MODELS

F.R. Yeatts

[1] *Professor Emeritus, Department of Physics, Colorado School of Mines, Golden, CO, USA*

Abstract. This study of tree morphology is presented in three parts: Part 1 deals with the profile (or envelope) of trees and woody plants. Noting that most trees exhibit: (i) azimuthal symmetry about the central axis (often the main stem or bole) in both in foliage and scaffolding; and (ii) decrease in leaf density from branch-end toward the central axis, a mathematical model is developed using the calculus of variations that predicts the profile, with but one free parameter. The analysis predicts profiles range from the nearly spherical in the case of uniform distribution of leaves throughout the crown, to essentially conical when the leaves are found largely on the branch-ends. The results are presented in figures showing theoretical profiles overlaid on photographs of representative trees.

Part 2 is based on field measurements that show that the cross-sectional area of a branch (or stem) entering a fork (in the direction of water transport) is *less than* the sum of the cross-sectional areas of the branches leaving that fork. Mathematical analysis using the calculus of variations shows that this "bulking up" actually *reduces* the quantity of plant tissue incorporated in the branching. Furthermore, it is shown that the angle of branching increases with bulking up. Field measurements are in rough agreement with this prediction.

Part 3 brings together the concepts of the first two parts to predict the cross-sectional area of the bole as a function of longitudinal position. Using equations appropriate to a tree with a single main stem and horizontal side branches, the cross-sectional area of the bole is calculated. The results compare favorably with field measurements.

Keywords: Morphology; Woody plants; Optimization; Calculus of variations

General Background

The primary objective of this report is to show how certain morphological characteristics of trees and other woody plants can be understood as strategies to minimize plant tissue. In particular the study addresses two general features: (1) the outline (envelope) or *profile* of trees, and (2) the *branching angles* exhibited at forks. The calculus of variations is used to address these problems. Field measurements were used to both motivate the study and to follow up on predictions of the theory. The study is concerned with "universal" properties of woody plants that transcend the peculiarities of species.

The paper is divided into three Parts: Part 1 deals with the profile of a tree. Based on the azimuthal symmetry of trees about a vertical axis and the requirements of photosynthesis, it is found that the distribution of leaves (photosynthetic units) is sufficient to determine the profile, from rounded to conical, with just one diagnostic parameter.

The Part 2 builds on the result (unexpected to this author) that the sum of the cross-sectional area of the branches leaving a fork is generally greater than the cross-sectional area of the branch feeding into the juncture. This result holds across all species measured. The analysis shows that this "bulking-up" provides for the most efficient branching.

Part 3 combines predictions of Parts 1 and 2 to provide a further check on the preceding results. Here, the cross-sectional area of the bole (for a tree with a single main stem) is determined as a function of vertical position No new concepts are introduced.

A search of the literature provided precious little for direct reference, but a wealth of background material. Beyond the specific works cited below, many prominent lines of research have addressed the problems of tree morphology and function. As a prime example, the pipe model theory, first proposed by Shinozaki et al. (1964),

hypothesized that a tree can be conceived as a bundle of pipes of fixed cross-section, some living some senescent; each living pipe connects a unit of foliage to the root system; each senescent pipe is retained as heartwood. Many elaborations and extensions followed. For example: Waring et al. (1982) used pipe theory to predict canopy leaf area. Valentine (1985) used it to study tree growth. Rennolls (1994) used it to investigate stem-profile. Makela (2002) used it to further study stem taper considering carbon balance. Valentine and Makela (2005) combined pipe theory with models for crown height, stem area, and carbon balance to better model tree growth and form.

Considering specific species and stands: Valentine et al. (1994) applied the pipe model to stands of Sitka spruce or loblolly pine; Makinen et al. (2003) and Berninger et al (2005) applied it to scots pine; Kantola et al. (2007) extended pipe model concept to a broader based model which they used to study Norway spruce.

West et al. (1997) proposed a comprehensive model (the WBE model) of plant structure based on a volume-filling fractal branching network, mechanical considerations, pipe model concepts, and 3/4 power allometric scaling law. Makela and Valentine (2006) showed how crown ratio influences scaling. More recently, Savage et al. (2010) upgraded the WBE model by considering trade-offs between hydraulic safety and efficiecy while incorporating more comprehensive empirical data.

Robin J. Tausch (2009) also proposed an analytical model for estimating biomass of tree crowns by considering the structural consequences of their physical and physiological requirements.

Statistical studies are also prominent in the literature: the work of Wang and Rennolls (2007) on the use of a bivariate distribution to model tree diameter and height illustrates this approach.

Part 1:

Profile

1.1 Introduction

The possibility of predicting the shape of a tree, the *profile* of its crown, from the distribution of its foliage was suggested to me by two general observations: (i) Most trees (at least in temperate latitudes) exhibit azimuthal symmetry, both in scaffolding and foliage, and (ii) the density of foliage is maximum near the stem or branch ends, decreasing inward toward the central axis.

Azimuthal symmetry, in the first place, implies that ambient, diffuse light alone is sufficient for the photosynthetic needs of the tree. (Indeed, photosynthesis saturates at 10 percent or less of direct sunlight (Emerson 1929, Hall and Rao 1999). The minor differences noted in the structure and function of leaves, north to south and top to bottom, might just as well be adaptations to protect the leaves from the direct rays, as adaptations to better utilize those rays.

In the second place, the decrease in leaf density is concurrent with the decrease in light intensity toward the interior region. (A simple study by the author using a photographic light-meter, was consistent with this qualitative expectation.) The explanation of how and why the distribution of foliage can exhibit azimuthal symmetry in spite of the asymmetric distribution of external light intensity is problematic to me; it is *as if* only ambient light matters.

For a given a distribution of foliage, I assume that the profile of a tree be that which maximizes the number of leaves on a tree of a given size. (Here, the term *leaf* is used as a proxy for a photosynthetic unit.) The four basic ingredients that control the growth of a tree are light, water, carbon dioxide, and nutrients. I assume that light alone is sufficient to determines profile. The corrupting effects of environmental factors, both external and internal, are neglected. The following theory thus applies to lone trees and woody plants privileged with optimum growing conditions.

The predictions of the model are in rough agreement with field observations. That is, trees with rounded profiles (like many deciduous species) tend to have foliage uniformly distributed throughout their crowns, while trees with conical profile (like many conifers) tend to have foliage concentrated near their stem ends. Figures 1.3a-d discussed below illustrate this agreement. I was unable to find any data on the radial density of foliage, so I relied on my own general observations.

Radar techniques such as were used by Tiangco and Forester (2000) to measure trunk-canopy biomass could, I believe, be adapted to radial density measurements. The use of stereo photos of tree crowns (Mitchell 1975b) might provide a better means of determining profiles.

Four prominent works have been of important to me in setting the stage for the present work:

Emerson (1929) provided some of the earliest measurements on photosynthesis as a function of light intensity. His work addressed chlorophyll concentration, wavelength of light (color), and rates of photosynthesis.

Horn (1971) was concerned with the succession of tree species from open field to climax forest conditions. Concentrating on available light, he modeled a tree as a multiply layered structure, each layer containing leaves ran-

domly distributed. By both calculating and measuring filtration of direct sunlight under various conditions, he was able to make predictions on crown shape ranging from conical, to ellipsoidal, to cylindrical (which he recognized as unlikely). He did not consider reflection thus ignored the possibility of diffuse light.

Hall and Rao (1999) provide a valuable compendium of photosynthesis from a history of our understanding the process to its biology and chemistry.

The more recent text by Thomas (2000) provides a comprehensive review of the natural history of trees from their geologic past, their form and function, to their care and nurturing. This resource was of particular value to me in understanding the physiology and anatomy of trees.

The text by Bell (1991) on *Plant Form* provides a highly detailed analysis and classification of plant forms. The section on "Plant branch construction" was of particular interest to me.

Mitchell (1975a) proposed a crown model with profile given by a logarithmic increase of branch size with distance from tree top, and foliage density constant to within a certain distance from branch ends. This model shares some features with the model presented herein, but the profile here is deduced from more fundamental considerations.

1.2 Theory

Consider a cylindrical coordinate system (r, z, θ) with its origin at the top of the tree and the z-axis directed down the main stem (or symmetry axis), r is directed radially outward, and θ is the azimuthal variable. The function $R(z)$ is the average radial distance from the symmetry axis to the stem-end; $r = R(z)$ defines the profile of the tree.

Let $n(r, z)$ define the density of leaves, i.e. the average number of leaves per unit volume representative of the tree. The total number of leaves N, assuming radial symmetry, is given by

$$N = 2\pi \int_0^z \int_0^{R[z]} n\,[r, z]\, r\; dr\; dz, \tag{1.1}$$

where Z is the distance down to the leaf-line, that is, to the approximate point where the foliage ends. The area A of the surface bounding the tree, as defined by the profile $R = R[z]$, can be written

$$A = 2\pi \int_0^Z \left(R'^2 + 1\right)^{\frac{1}{2}} R dz, \tag{1.2}$$

where $R' = \frac{dR}{dz}$. The area A is taken as the (constant) measure of size.

The procedure followed below utilizes the calculus of variations to find the the function $R[z]$ which maximizes N for a given A. But first, it is necessary to introduce a density function $n[r, z]$ which satisfies the general requirements:

1. $n[r, z]$ is defined on the domain $0 < z < Z$, and $0 < r \leq R[z]$
2. $n[r, z] \leq n[R[z], z]$

A physically reasonable function which satisfies these requirements is given by

$$n\,[r, z] = n_1 \exp\left[-b\left(R\,[z] - r\right)\right], \tag{1.3}$$

where n_1 = constant. Equation (1.3) describes an exponential drop-off in leaf density from its maximum at $R = R[z]$. (This density function can be derived by assuming that, first, the tree is immersed in a uniform ambient light bath; and, second, that light intensity is reduced in proportion to the density of leaves intercepted (as in the Beer-Lambert law); and third, that the density of leaves at any point is proportional to the intensity of light at any point.) Two other density functions, one providing a linear fall-off and the other an error function fall-off were tried; both led, qualitatively, to the same results.

Equation (1.1) for N can now be readily integrated over r, thus:

$$N = \frac{2\pi n_1}{b^2} \int_0^Z \left(\exp\left[-bR\right] - 1 + bR\right) dz. \tag{1.4}$$

The specific function $R = R[z]$ which yields maximum leaf number N subject to the condition that A is constant is determined by the Euler-Lagrange (EL) differential equation:

$$\frac{d}{dz}\left(L - R'\frac{\partial L}{\partial R'}\right) = \frac{\partial L}{\partial z}, \tag{1.5}$$

where $R' = \frac{dR}{dz}$. The Lagrangian L, in turn, is given by the integrand of (1.4) added to (or subtracted from) λ, an undetermined multiplier times the integrand of the area constraint A of (1.2),

$$L = \exp\left[-bR\right] - 1 + bR - \lambda R\sqrt{R'^2 + 1}; \tag{1.6}$$

the constants multiplying the integrals (1.2) and (1.4) are subsumed in λ. Substitution of (1.6) into EL yields the differential equation

$$\frac{dR}{dz} = \left(\left(\frac{\lambda R}{\exp\left[-bR\right] - 1 + bR}\right)^2 - 1\right)^{\frac{1}{2}}. \tag{1.7}$$

The profiles displayed in Figures 1.3a-d were all obtained by a second order numerical integration of (1.7).

Two special cases of (1.7) are easily solved analytically: The first case, $bR \ll 1$, is satisfied by small r and/or small b; here, the exponential can then be approximated by $\exp[-bR] \approx 1 - bR + \frac{(bR)^2}{2}$. Equation (1.7) reduces to

$$\frac{dR}{dZ}\left(\left(\frac{\frac{2\lambda}{b^2}}{R^2} - 1\right)\right)^{\frac{1}{2}}, \tag{1.8}$$

which can be readily integrated to read,

$$R^2 + \left(\frac{2\lambda}{b^2} - z\right)^2 = \left(\frac{2\lambda}{b^2}\right)^2, \tag{1.9}$$

where $R = 0$ at $z = 0$. Equation (1.9) can be recognized as the formula for a circle of radius $\frac{2\lambda}{b^2}$ with center on the z-axis at $z = \frac{2\lambda}{b^2}$. For the condition $bR \ll 1$ to hold for all R, b itself must be very small; from (1.3), this implies that the exponential must be very slowly decreasing. Thus, a uniform distribution of foliage implies a spherical crown.

If $bR \gg 1$, then the exponential term $\exp[-bR]$ in (1.7) as well as the number 1, becomes negligible compared with bR. Thus, (1.7) reduces to

$$\frac{dR}{dz} = \left(\left(\frac{\lambda}{b}^2\right) - 1\right)^{\frac{1}{2}}, \tag{1.10}$$

whose integral, with $R = 0$ at $z = 0$, can be written

$$R = z\sqrt{\left(\frac{\lambda}{b}\right)^2 - 1}, \tag{1.11}$$

which represents straight lines passing through the origin with slopes $\sqrt{\left(\frac{\lambda}{b}\right)^2 - 1}$. A very large value of b implies a very large rate of fall-off of density from stem ends. Thus, foliage is concentrated near the stem-tips when the profile is conical.

Before comparing the theoretical results obtained from (1.7) with the profiles of actual trees, it is convenient to introduce the dimensionless variables: $\mathfrak{R} = bR$, $\mathfrak{z} = bz$, and $\mathfrak{c} = \frac{\lambda}{b}$. In terms of these variables, (1.7) can be written, after factoring the expression under the radical,

$$\frac{d\mathfrak{R}}{dz} = \left[\left(\frac{\mathfrak{c}\mathfrak{R}}{\exp[-\mathfrak{R}] - 1 + \mathfrak{R}} - 1\right) \times \left(\frac{\mathfrak{c}\mathfrak{R}}{\exp[-\mathfrak{R}] - 1 + \mathfrak{R}}\right) + 1\right]^{\frac{1}{2}} \tag{1.12}$$

The reduced variables $\mathfrak{R}$, $\mathfrak{z}$, and $\mathfrak{c}$ will be used in all that follows; note that $\mathfrak{c}$ is the only free parameter. The bounded solutions are now characterized by $\mathfrak{c} < 1$, and the unbounded by $\mathfrak{c} > 1$. Note also, that for real-valued solutions,

$$\mathfrak{c}\mathfrak{R} \geq \exp[-\mathfrak{R}] - 1 + \mathfrak{R}, \tag{1.13}$$

where, from (1.12), the equality holds for stationary points, $\frac{d\mathfrak{R}}{d\mathfrak{z}} = 0$. Figure 1.1 provides a graph of (1.12) for various values of the parameter $\mathfrak{c}$. Note that, for $\mathfrak{c}$ ¿ 1,

$$\lim_{\mathfrak{R}\to\infty}\left(\frac{d\mathfrak{R}}{d\mathfrak{z}}\right) = \sqrt{\mathfrak{c}^2 - 1} \equiv \tan\alpha. \tag{1.14}$$

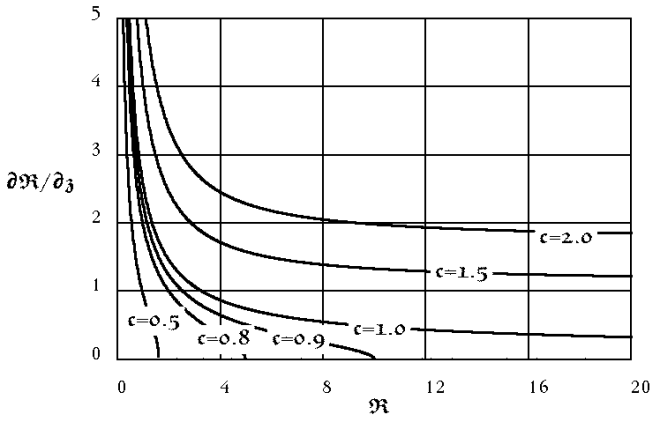

Figure 1.1: Graphs of $\frac{d\mathfrak{R}}{d\mathfrak{z}}$ versus $\mathfrak{R}$ for various values of $\mathfrak{c}$ from equation (1.12). For cases where $c < 1$, $\frac{d\mathfrak{R}}{d\mathfrak{z}} = 0$ gives the radius $\mathfrak{R}_M$ of maximum girth. For $\mathfrak{c} > 1$, the *horizontal asymptote* of $\frac{d\mathfrak{R}}{d\mathfrak{z}}$ equals the tangent of the half-angle α of the enveloping cone, as in (1.14).

Numerical integration of (1.12), evaluated at the limit $\frac{d\mathfrak{R}}{d\mathfrak{z}}$=0, enables one to calculate the $\frac{\mathfrak{R}_M}{\mathfrak{z}_M}$ versus $\mathfrak{c}$ at maximum girth. The results are shown in Figure 1.2.

In general, the solutions to (1.12) bear a striking resemblance to the conic sections. For values $\mathfrak{c} < 1$, the solutions are approximately elliptical, depicting crowns that are "pseudo-ellipsoidal". The solutions are slightly broader near the vertices than their conic counterparts. For values $\mathfrak{c} > 1$, the solutions are hyperbolic depicting crowns that are "pseudo-hyperboloids " (one sheet of the two-sheet variety). The asymptotes define the conical appearance in this case. For $\mathfrak{c} = 1$, the "parabolic" case, the crown appears cylindrical with a rounded top. (Unlike the parabola, the derivative $\frac{d\mathfrak{R}}{d\mathfrak{z}} = 0$ for large $\mathfrak{z}$.)

1.3 Experimental Results

Digital images of a number of trees and woody shrubs were acquired using a Panasonic Lumix (DMC FZ35) camera in telephoto mode. Each image was cropped,

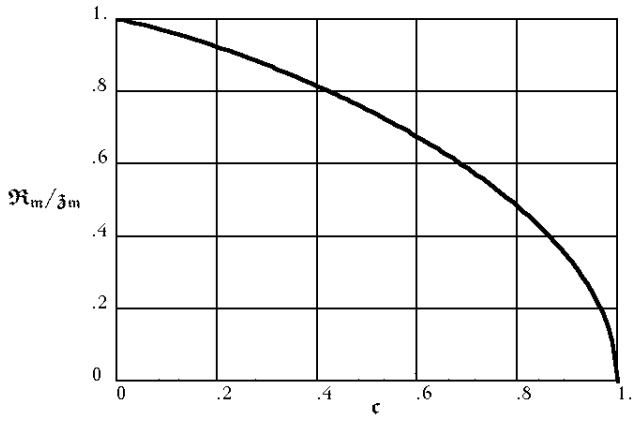

Figure 1.2: Graph of $\frac{\mathfrak{R}_M}{\mathfrak{z}_M}$ versus $\mathfrak{c}$ for the elliptic case, $\mathfrak{c} < 1$. From (1.12) , values of $\frac{\mathfrak{R}_M}{\mathfrak{z}_M}$ where computed for $\mathfrak{c} = 0.0, 0.2, \ldots, 1.0$. A smooth curve was drawn through these points.

if necessary, and down-loaded into a True BASIC program designed to superimpose a computed profile over the tree. Examples of four such "best fits" are shown in Figures 1.3 (posted at the end of Part 1). In my research, 33 trees and woody shrubs were thus studied. The trees chosen for inclusion in this report are not exceptional; they were selected mainly to exemplify the various of tree shapes. Of course, only uncrowded, undamaged, mature trees were included in the study. To minimize parallax, unobstructed views were required so as to obtain telephoto images.

The trees included in this report include two Honey-locust *Robinia pseudoacacia*, Spruce *Picea engelmannii*, and Juniper *Juniperus scopulorum*. Superimposed on each image is the "best fit" theoretical profile matched by adjusting the constant c and the position of the leaf-line $\mathfrak{z}_N$. The "best fit" profiles were determined by "eye". (A numerical scheme such as "least-squares" could have been used, but in this author's opinion, such analysis is not warranted in this preliminary study with limited data.) Also shown on those figure for which $\mathfrak{c} < 1$, is the coordinates of maximum girth, $\mathfrak{z}_M$. The best-fit values of this analysis are given in Tab 1.1 to two significant figures of accuracy.

The leaf-line constant $\mathfrak{z}_N$ was introduced originally to limit the range of numerical integration. However, this constant is somewhat diagnostic of tree shape for conifers. For the set of spruce trees studied, $c \approx 0.9$, and moreover $\frac{\mathfrak{R}_N}{\mathfrak{z}_N} \approx 0.3$. No analogous relationship was observed among deciduous trees; contrarily, note the difference in c values between the two honey-locust trees in Table 1. For trees with $c > 1$, the parameter $\mathfrak{z}_N$ is particularly relevant to tree shape: the greater $\mathfrak{z}_N$, the "sharper" the tree top.

The parameter b associated with the decrease in leaf density with distance in from branch-end can be evaluated using the scaling relations $\mathfrak{R} = bR$ and $\mathfrak{z} = bz$ introduced just above equation (1.12). The coordinate of maximum girth, $\mathfrak{R}m$, is particularly convenient (when $\mathfrak{e} < 1$) because it can be computed directly from (1.13) at equality.

The computed values b are generally higher than expected: $\frac{1}{b}$ implies a "compensation point" where leaf density is decreased by $\frac{1}{e} \approx 0.368$ of its maximum value at branch-end. By measurement, in several cases, the actual distance $\frac{1}{b}$ is greater than that calculated and shown in Tab. 1.1.

1.4 Discussion and Summary

The approximate azimuthal symmetry common to most trees in this temperate latitude (Colorado) suggested to this author that growth and form progress *as if* ambient light alone is sufficient.. Building on this concept, and using the density of foliage as a proxy for the distribution of photosynthetic units, a theory was developed which determines the profile of a tree (crown) from optimization of the light gathering potential, i.e. the number of leaves available.

The theory predicts, reasonably well, the profile of trees: generally, trees with uniform distribution of foliage exhibit rounded crowns (such as with many deciduous tree); trees with their foliage concentrated near the outer stem-ends exhibit conical crowns (such as with many conifers). Mathematically, the calculus of variations was used to find the profile (i.e. the radial branch length as a function of position along the main stem symmetry axis) which gave the maximum number of leaves (the integral of the leaf density) for a given size of tree (as measured by a fixed bounding surface area). A density-of-foliage function was introduced that held the stem-end leaf density constant, and allowed a fall-off of density inward toward the main stem or symmetry axis. An exponential density function was chosen which met these requirements.

The theory also predicts that the single parameter, c (> 0) is sufficient to define the profile. Trees with $c < 1$ have rounded profiles ($c = 0$ are circular); with $c > 1$, conical. The profiles are qualitatively similar to the conic sections: Indeed, the terms *elliptic*, and *hyperbolic* serve as appropriate bynames for the respective profiles, overlooking the sometimes significant quantitative differences.

The theory was compared with actual trees by superimposing the computed profiles over the digital images of actual trees. Beyond adjusting for scale by setting z_N at "leaf-line", only the parameter c was varied to make

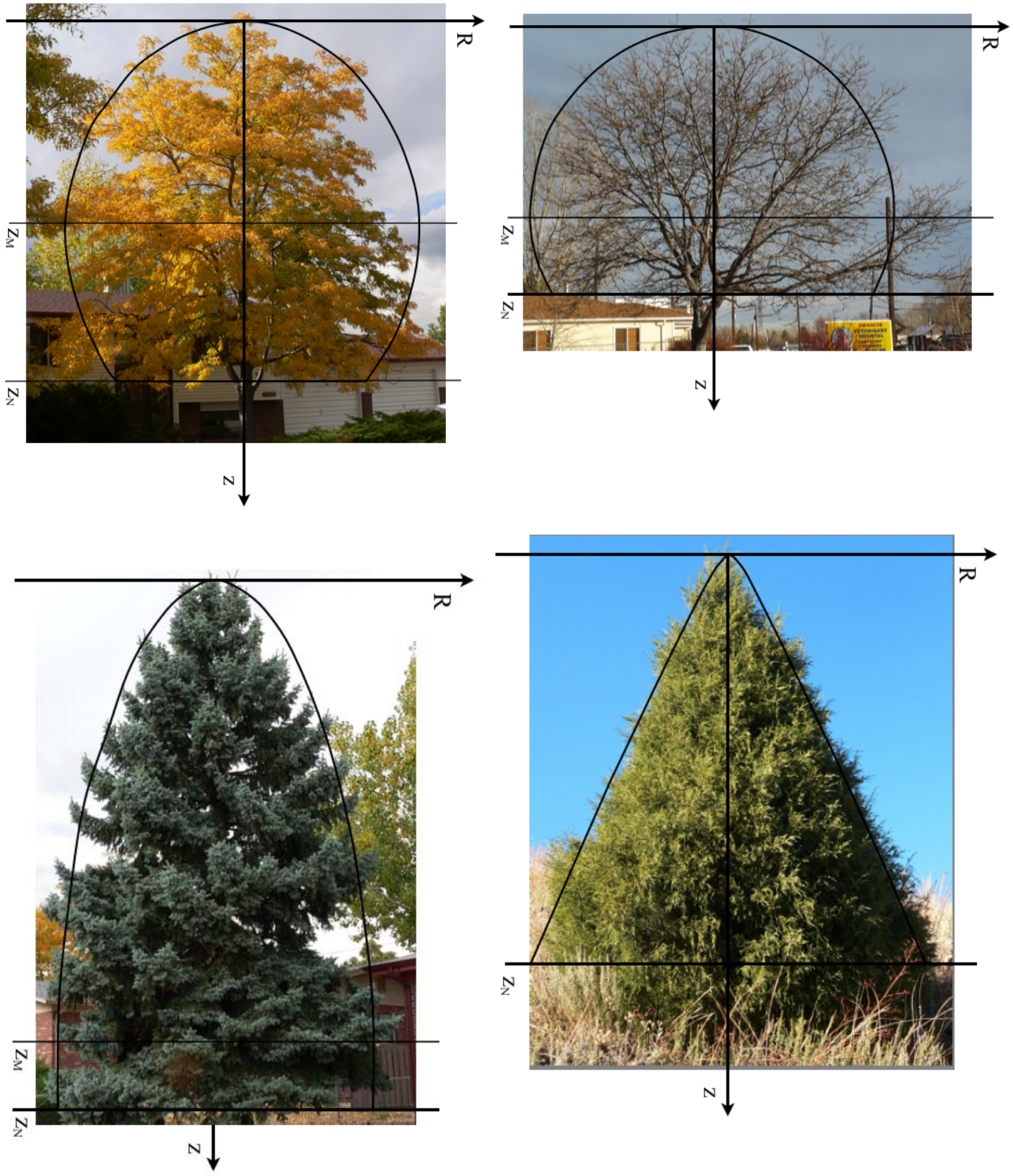

Figure 1.3: Photographs of trees with computed profiles superimposed. Upper left. Honey-locust *Robinia pseudoacacia* ($\mathfrak{c} = 0.6$). Upper right. Honey-locust *Robinia pseudoacacia* ($\mathfrak{c} = 0.1$). Lower left. Spruce *Picea engelmannii* ($\mathfrak{c} = 0.9$). Lower right. Juniper *Juniperus scopulorum*, ($\mathfrak{c} = 1.1$)

Tree	$\mathfrak{c} \pm \Delta\mathfrak{c}$	$\mathfrak{z}_N$	$\mathfrak{R}_N$	$\mathfrak{z}_M$	$\mathfrak{R}_M$	$(1/b)[cm]$
Honey-locust	0.6±0.1	6.0	2.1	3.7	2.9	200
Honey-locust	0.1±0.1	0.3	0.2	0.2	0.2	3700
Spruce	0.90±0.05	35	9.9	31	10	2
Juniper	1.1±0.1	70.0	196.0	NA	NA	0

Table 1.1: "Best fit" values of c and the associated values, $\mathfrak{z}_N$, $\mathfrak{R}_N$, $\mathfrak{z}_M$, $\mathfrak{R}_M$, and b. The uncertainty values $\pm\Delta\mathfrak{c}$ indicate the range over which $\mathfrak{c}$ can be adjusted with less than 10% change in the values of the other parameters.

a good visual fit. I also found that, for trees for which $c < 1$, the ratio $\frac{R_M}{z_N}$, where z_M is the longitudinal position of maximum girth, is rather constant for a given species; this relationship was not investigate further in this study. In a similar manner, for conical trees, the setting of z_N adjusted for the roundedness of the tree apex, high settings of z_N gave pointed apices.

The agreement between the distribution of leaves and the availability of light (which was the concern motivating this study) was not determined because of my not having convenient way of measuring both leaf density and light intensity within the crown. I tried to determine leaf density by measuring the light passing through the foliage using a light meter-telescope combination, but this strategy was not successful.

It is well known that the tree-growth is controlled the four basic ingredients: light, water, carbon dioxide, and nutrients. The present study suggests that light alone is responsible for tree shape (although I admit that the connection of light to foliage was not well established in this study). But further evidence of this hypothesis follows from the observation that a tree with multiple main stems, or even a small group of trees growing very close together, produce a collective crown whose profile is similar to that of a single tree.

Part 2:

Branches

2.1 Introduction

This study is based on one simple but significant observation: The cross-sectional area of a branch (or stem) entering a fork (in the direction of water transport) is less than the sum of the cross-sectional areas of the branches leaving that fork. To quantify this, I introduce the "bulking ratio"

$$\gamma \equiv \frac{\text{Area.of.branch.entering.fork}}{\sum \text{Areas.branches.leaving.fork}} \qquad (2.1)$$

All areas are measured outside of the swollen region (collar) of the fork. I made measurement on 128 forks on 21 different species of trees and tall shrubs, chosen opportunistically, in the vicinity of Denver, CO. To my surprise, the mean bulking ratio was less than one: indeed, $\gamma_{\text{av}} = 0.867$ with standard deviation $\text{SD}_\gamma = 0.105$. The probability of this result if γ_{true}=0 is clearly infinitesimal.

Moreover, and even more surprising to me, was a relationship between γ and the angles between the outgoing branches: *The angles between the out-going branches tended to increase with* γ. The primary objective of this Part is to understand this relationship.

One might expect that the ratio of areas should be *one* considering both the continuity of venation across the fork and the strength required to support the weight-of-branch beyond the fork. In this latter regard, the cross-sectional area of a branch (or stem) at a given point is proportional to the load supported at that point. The constant of proportionality depends on the strength of the wood. (Specifically, the strength required depends on whether the wood at that point is under compression, tension, torsion, flexure, or some combination there of.) Strength is measured in units of *force per unit area*. It is assumed that the swollen region of the fork is sufficiently small (in distances along the branches) that the load supported by the incoming branch is essentially the same as that supported by the sum of the outgoing branches.

2.2 Theory

To simplify the analysis, considere a *simple* two-branched fork confined to a single plane; see Figure 2.1. The line QO represents the incoming branch; OP and OP' the outgoing branches. The lines QO, OP, and OP' lie in a single plane. The ellipses at the ends of the outgoing branches represent terminal buds. The angle $\omega = \theta_\omega + \theta_\omega{}'$ is the only angle measured in the field; the other angles as well as the lengths r, s, s', t, and t' are used in the analysis. A fork in which the branches OP and OP' lie in a different plane from that of QO and OP requires three independent angles. A *three-branched* fork, for comparison, has five independent angles; inclusion of such forks complicates both the analysis and the field measurements.

The fork, as introduced, concerns terminal twigs. The analysis, however, reduces to a consideration of the fork in the *neighborhood* of point O, at which only the *areas* of the incoming and outgoing branches are involved. Because it seems reasonable (and not contradicted by limited observations) that a fork maintains its geometry from inception to maturity, the analysis is assumed valid for all simple forks.

My strategy is to assume some reasonable model for the cross-sectional area of a branch in terms of position along the branch, then, given the positions of the positions Q, P, and P', find the point O that minimizes the volume of tissue in that region of fork. The points P, P', and Q are merely reference points which, it will be shown, drop out in the final analysis.

As the two branches are usually of different sizes, I introduce the *branching ratio* χ.

$$\chi \equiv \frac{\text{Area.of.smaller.branch.leaving.fork}}{\text{Area.of.large.branch.leaving.fork}} \tag{2.2}$$

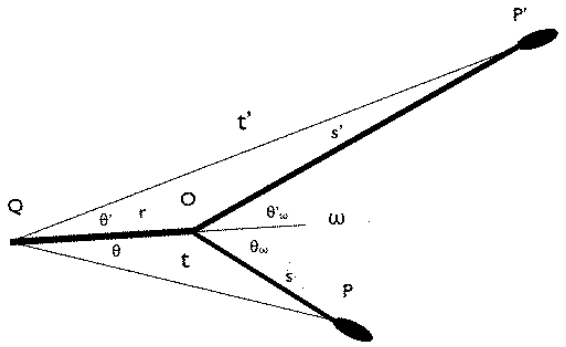

Figure 2.1: The geometry associated with the analysis of the fork. Point O locates the intersection of the central lines of the branches. Point Q is a point on the center-line of the incoming branch arbitrarily close to point O. Points P and P' on the center-lines of the out-going branches denote positions of equal branch area; P and P' are arbitrarily close to point O.

The volume V of a branch segment (with no intervening side branches) between points a and b can be written as the integral of the branch area $A[x]$ in terms of the distance x is along the branch,

$V = \int_a^b A[x]dx$. It is convenient to write the area as the product $A[x] = A_0 g[x]$ such that $g[0] = 1$; it is reasonable to think of $g[x]$ as a monotonically increasing function of x. In the case of constant elastic modulus, $g[x]$ would be exponential: $g[x] = \exp[bx]$, where x is measured inward/downward. Choosing points P and P' (terminal branch ends) as the starting points along the two outgoing segments OP and OP', their volumes are, respectively,

$$V_s = A_0 \int_0^s g[x]dx = A_0 G[s], \tag{2.3a}$$

$$V_{s'} = A_0 \int_0^{s'} g[x]dx = A_0 G[s'], \tag{2.3b}$$

where capital G refers to the integral g. Here, $G[x]$ must be differentiable, $\frac{dG}{dx} = g[x]$. I assume that the area of the branch at point P is the same as that at P'!

The volume of the segment QO is given by

$$V_r = A_1 \int_0^r g[x]dx = A_1 G[r], \tag{2.3c}$$

where A_1 is the area of the incoming branch measured at point O. From the definition of the bulking constant (2.1), one can write

$$A_1 = \gamma(A_s + A_{s'}) = \gamma A_0 \left(g[s] + g[s']\right). \tag{2.4}$$

Thus, the expression for the volume V_r can be written

$$V_r = A_1 \int_0^r g[x]dx = \gamma A_0 \left(g[s] + g[s']\right) G[r].$$

The total volume of the fork $V = Vs + Vs' + Vr$, where the volume of the swollen part of the fork is neglected. From equations (2.3a, 2.3b 2.3c),

$$V = A_0 G[s] + A_0 G[s'] + \gamma A_0 \left(g[s] + g[s']\right) G[r]. \tag{2.5}$$

The distance s and s' can be related to r, θ and r, θ' by means of the cosine theorem as applied to the triangles of Figure 1:

$$s^2 = t^2 + r^2 - 2rt\cos\theta, \tag{2.6a}$$

$$s'^2 = t' + r^2 - 2rt\cos\theta'. \tag{2.6b}$$

The minimum of V, then, is determined by the conditions $\frac{\partial V}{\partial r} = 0$ and $\frac{\partial V}{\partial \theta} = 0$. Thus, from (2.5), and

recalling that $\frac{dG}{dx} = g[x]$:

$$\frac{\partial V}{\partial r} = A_0 \left(g[s]\frac{\partial s}{\partial r} + g[s']\frac{\partial s'}{\partial r} + \gamma \left(g[s] + g[s'] \right) g[r] + \right.$$
$$\left. + \gamma \left(\frac{dg}{ds} + \frac{\partial s}{\partial r} + \frac{dg'}{ds'}\frac{\partial s'}{\partial r} \right) G[r] \right), \tag{2.7a}$$

$$\frac{\partial V}{\partial \theta} = A_0 \left(g[s]\frac{\partial s}{\partial \theta} + g[s']\frac{\partial s'}{\partial \theta} + \right.$$
$$\left. + \gamma \left(\frac{dg}{ds}\frac{\partial s}{\partial \theta} + \frac{dg'}{ds'}\frac{\partial s'}{\partial \theta} \right) G[r] \right). \tag{2.7b}$$

The partial derivatives of s and s', here, can be calculated from the cosine theorems (2.6a, 2.6b); again, with reference to Figure 2.1,

$$\frac{\partial s}{\partial r} = \frac{r - t\cos\theta}{s} = -\cos\theta_\omega, \quad \frac{\partial s}{\partial \theta} = \frac{rt\sin\theta}{s} = r\sin\theta_\omega, \tag{2.8a}$$

$$\frac{\partial s'}{\partial r} = \frac{r - t\cos\theta'}{s} = -\cos\theta'_\omega, \quad \frac{\partial s'}{\partial \theta} = \frac{rt'\sin\theta'}{s'} = r\sin\theta'_\omega. \tag{2.8b}$$

Consider (2.7a, 2.7b) in the limit of very short incoming branch, i.e. $r \to 0$; in this limit, $g[r] \to 1$ and $G[r] \to 0$. Equations (2.7a, 2.7b), with (2.8a, 2.8b), can be written,

$$\frac{\partial V}{\partial r} = A_0 \left(g[s](-\cos\theta_\omega) + g[s'](-\cos\theta'_\omega) + \right.$$
$$\left. + \gamma(g[s] + g[s']) \right), \tag{2.9a}$$

$$\frac{\partial V}{\partial r} = A_0 \left(g[s]\sin\theta_\omega - g[s']\sin\theta'_\omega \right) r. \tag{2.9b}$$

Ignoring the trivial solution $r = 0$ in (2.9b), setting $g[s] + \chi g[s']$, (following (2.2), and recognizing that $A_0 g[s]$ and $A_0 g[s']$ are the areas of the outgoing branches near point O, factoring out the term $g[s']$, and setting the derivatives equal to zero , one finds:

$$\gamma(\chi + 1) - \chi\cos\theta_\omega - \cos\theta'_\omega = 0, \tag{2.10a}$$

$$\chi\sin\theta_\omega - \sin\theta'_\omega = 0. \tag{2.10b}$$

Equations (2.10b) can be solved simultaneously for θ_ω, and θ'_ω. By squaring and converting the sines to cosines, and performing the required algebra:

$$\cos\theta_\omega = \frac{1}{2\chi}\left((1+\chi)\gamma - (1-\chi)\frac{1}{\gamma} \right), \tag{2.11a}$$

$$\cos\theta'_\omega = \frac{1}{2\chi}\left((1+\chi)\gamma - (1-\chi)\frac{1}{\gamma} \right). \tag{2.11b}$$

Also, with reference to Figure 2.1,

$$\omega = \theta_\omega + \theta'_\omega. \tag{2.12}$$

Equations (2.11a, 2.11b) and (2.12) can be solved numerically to give ω as a function of γ and χ. Figure 2.2 provides graphs of ω versus χ for several appropriate values of γ. Note the limits:

- For $\gamma = 1$ (no area increase across the fork), $\theta = \theta' = 0°$, thus $\omega = 0°$. In this case there would be no branching at all; every leaf would find itself on a lone stem originating at the ground.
- For $\chi = 1$ (equal size branches leaving the fork), equations (2.11a, 2.11b) yield $\theta = \theta' = \cos^{-1}\gamma$, thus, from (2.12),

$$\omega = 2\cos^{-1}\gamma. \tag{2.13}$$

  This formula (by inspection of Figure 2.2) holds to fair approximation for branching ratios $\chi > 0.6$.
- There is a minimum branching ratio $\chi_{\min}$ for any given bulking ratio γ,

$$\chi_{\min} = \frac{1-\gamma}{1+\gamma}. \tag{2.14}$$

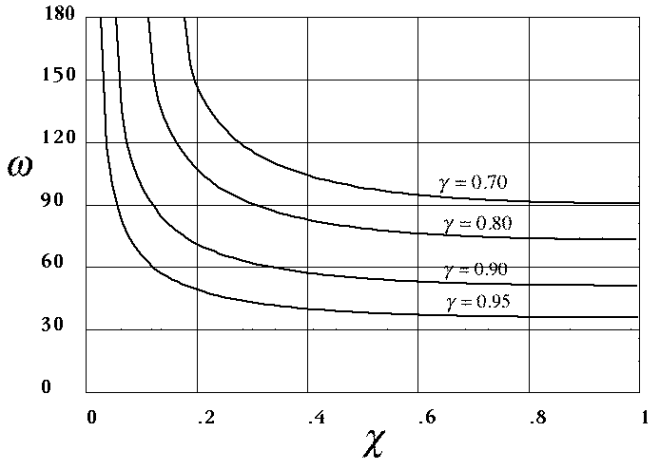

Figure 2.2: A graph of the branching angle ω versus the branching ratio χ for four different values of the bulking ratio γ. The equal-branch ($\chi = 1$) solution, $\omega = 2\cos^{-1}\gamma$, holds approximately for $\chi > 0.6$.

Equation (2.11a) shows that the angle θ_ω increases with decreasing χ, while (2.11b) shows that θ'_ω decreases with decreasing χ, both as expected. Moreover, as χ becomes small (think twig) the corresponding bulking

ratio γ must approach *one* (even branching), again as expected.

For the case of small χ, branching angles $\omega > 90°$ is curious; it suggests that a twig can be reflexed i.e. angled back on its incoming branch. Either this is an unrealistic artifact of the theory, or perhaps it allows for the unusual case that ample light is found in the interior regions of the tree promoting reflexed behavior? It is this author's intention to pursue this matter.

Consider a branch segment as shown in Figure 2.1 with the incoming branch starting at point Q, the *optimized* branch point at O, and the outgoing branch ends at points P and P'. From Figure 2.2, the volume V (as given in (2.5)) is a monotonically increasing function of the bulking ratio γ, for given value of χ. This implies that less volume of wood is needed to connect point Q with P and P' if the bulking up is low; thus, the branching angle high.

2.3 Field Measurements

Prior to conducting the theoretical work described in the preceding section, I measured the cross-sectional areas of the incoming and outgoing branches of 124 forks representing 21 species of trees and tall shrubs near Denver, Colorado. In terms of the ratio bulking ratio defined in (2.1), I found that, $\gamma_{\rm av} \pm \Delta\gamma = 0.877 \pm 0.105$, where 0.105 is the standard deviation. The probability that the population mean $\gamma^*_{\rm av} = 1$, given my data, is infinitesimal.

The only requirement I imposed on the specimens was that all the branches be relatively round so that the circumference *squared* would serve as a proxy for area. (To measure the circumferences I used a flexible measuring tape wrapped just beyond the swollen region of the fork.) Fortunately, 103 of my earlier measurements were "simple" forks for which I had also measured (with a large two-armed protractor) the branching angle ω. It was surprising to me, incidentally, how few forks were of this simple two-branched variety. Most forks involved three or more out-going branches, some forks were within the swollen zone of neighboring forks, and some forks were simply not round enough or too disfigured to qualify. I measured forks with circumferences ranging from a few millimeters to meters. Where possible, I would select forks on recently dead branches without bark so as to focus attention on supportive tissue alone.

I did not attempt to collect a scientifically random sample; I just selected trees and shrubs of as many different species which were convenient for me to measure. I did not distinguish between forks in branches, branches off the main stem, or bifurcations of the main stem. Because I am interested in "universal" properties of woody plants, I sampled as broad a representation of species and sizes as possible. My data set is not large enough to distinguish quantitatively agreement within species or differences between species, although I have noted some such regularities.

Figure 2.3 shows a graph of branching angle ω versus bulking ratio γ for forks with out-going branch area ratio $\chi > 0.6$. Forks with $\chi > 0.6$ (somewhat equally sized out-going branches) obey, approximately, (2.13).) Here, 76 of the 103 specimens meet this criterion.

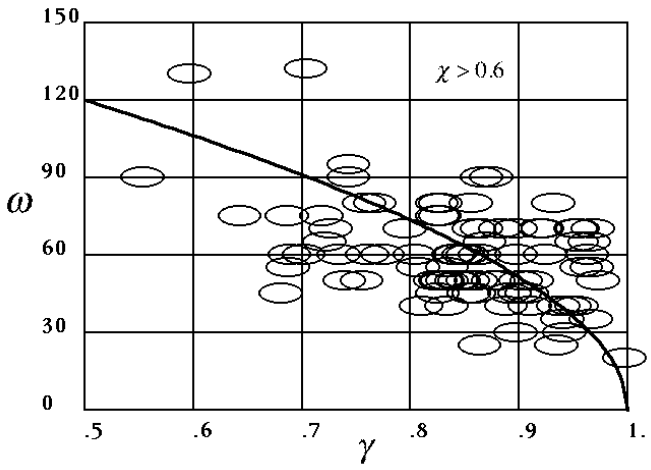

Figure 2.3: A graph of the measured values of the branching ratio ω versus the bulking ratio γ for 76 specimen of trees and shrubs of branching ratio $\chi > 0.6$. The data is represented by ellipses whose dimensions gives the average measurement error. The smooth curve gives the theoretical dependence $\omega = 2\cos^{-1}\gamma$.

The trend of the data is in agreement with the theory, but the spread is too great to make any meaningful comparison with theory. This spread might well be due to environmental factors affecting the forking. Moreover, with regard to theory, the *minimum* in volume, from which the theoretical branching angle is determined, is both broad and shallow. This means that there is little penalty in tree resource if the optimum branching angle is not achieved. (Perhaps the curve of ω versus γ should be drawn with a broad pen.)

On the other hand, environmental factors alone could account for the spread of the data about the theoretical curve. From field observation, considerable variation in both γ and ω can be seen within a given tree as well as between trees of the same species. Indeed, the variation of branching angle within a species is often as great as the difference between species. Considerably more data is needed to elucidate possible systematic relationships between γ and ω. Longitudinal sectioning of a few (eight) forks revealed that the branching angle as measured at the pith lines is generally the same as the angle measured with whole branches.

2.4 Discussion and Summary

The "bulking up" of branches, as measured by γ seems to be an empirical fact, at least for the vast majority of trees and woody shrubs in this temperate zone. Likewise, the increase in branching angle ω with increasing γ is strongly suggested. It is reasonable to believe that branching angle is genetically controlled; my measurements on young sprouts (not included in this report) show significant variation around the average. Perhaps those branches that are favorably oriented have a better chance of surviving to maturity and being measured by a curious researcher.

The value of this study to conventional tree architecture is in the constraints it imposes on branching. But with respect to understanding the morphological implications of genetic control, this work could provide a theoretical framework. As the branching angles were measured on relatively mature trees, environmental factors have had time to operate. Perhaps sectioning more branches longitudinally (as advocated by Shigo (1994)) through the forks and measuring the initial branching angles at the core (point O in Fig. 2.1) would be more appropriate.

This author is under no illusion that the theory presented here provides the primary explanation of fork morphology. There is, however, strong empirical evidence that "bulking up" occurs and that branching angle ω is related to the bulking ratio γ . The minimum volume theory presented here provides a plausible explanation for that relationship.

Part 3:

Trunk

3.1 Introduction

The objective of this Part is to exploit the concepts of the first two Parts of the report to further test of the validity of those ideas. In particular, the shape of the main stem (i.e. the cross-sectional area of the main stem as a function of position) is deduced from the profile of the tree and the angle of branching off the main stem. This study is limited to trees with a single main stem whose primary branches make an angle of 90 degree with the trunk. The theoretical results, then, are compared with actual measurements on three representative trees: a douglas-fir (*Pseudotseuga menziesii*), a juniper (*Juniperus scopulorum*), and an aspen (*Populus tremuloides*). As this study is intended merely as a check on the preceding studies, no effort was made to include a greater number of individuals or a broader variety of species. (Trees featuring both a single main stem and perpendicular branching limited the number of species available, especially among deciduous trees.)

3.2 Mathematical Set-up

The average behavior of branches off the main stem can be modeled as a distribution of infinitesimal branches, each originating at the axis of the main stem, projecting perpendicular from the axis to a terminal point at coordinate r, θ, z, where one can imagine an infinitesimal leaf. Assuming exponential increase of branch area towards the main stem, and a terminal branch area proportional to the density of leaves at that point, the element of cross-sectional area d^3a at the main stem (approximated as $r = 0$) can be written

$$d^3a \propto \exp[\alpha r] \exp\left[-b(R[z] - r)\right] r dr d\theta dz, \qquad (3.1)$$

where $R[z]$ gives the profile as defined in Part 1; α and b are constants as defined previously. Expression (3.1) can be integrated first over θ (the partial integral being 2π) and then over r to yield.

$$da = \frac{Cb}{(\alpha + b)^2}\big(\left((\alpha + b)\, R - 1\right) \exp[\alpha R] + \\ + \exp[-bR]\big) dz, \qquad (3.2a)$$

where $R = R[z]$ and C is a constant.

With the introduction of the dimensionless variables defined above Equation (1.12): (3.2a) can be written

$$da = C\frac{1}{(1 + \mathfrak{e})^2}\big(\left((1 + \mathfrak{e})\, \mathfrak{R} - 1\right) \exp[\mathfrak{e}\mathfrak{R}] + \\ + \exp[-\mathfrak{R}]\big) d\mathfrak{z}, \qquad (3.2b)$$

where, again, $\mathfrak{z} = bz$, $\mathfrak{R} = bR$, and $\mathfrak{e} = \frac{\alpha}{b}$, $\mathfrak{a} = b^2 a$, and $\mathfrak{R} = \mathfrak{R}[\mathfrak{z}]$.

As applied to the fork formed by the main stem and the infinitesimal branch intersecting at a length element dz, the bulking ratio γ (equation (2.1) is given by

$$\gamma = \frac{A[z + dz]}{A[z] + da} = \frac{A[z] + \frac{dA}{dz} dz}{A[z] + \frac{da}{dz} dz} = 1 - d\gamma, \qquad (3.3)$$

where

$$d\gamma = \frac{1}{A}\left(\frac{da}{dz} - \frac{dA}{dz}\right) dz \qquad (d\gamma \geq 0). \qquad (3.4)$$

Tree	$\mathfrak{c}$	$(1/\mathfrak{b})$[cm]	$\mathfrak{R}[\mathfrak{z}]$	$\mathfrak{e}$	$\mathfrak{C}$	$\sqrt{\text{variance}}$
Juniper	1.11	2	$0.5\mathfrak{z}$	0.012	$6.6*10^{-3}$	0.02
Aspen	0.88	25	$0.36\sqrt{46\mathfrak{z}-\mathfrak{z}^2}$	0.04	$1.0*10^{-4}$	0.04
Douglas-fir	0.99	3.5	$.093\sqrt{2160\mathfrak{z}-\mathfrak{z}^2}$	0	$1.15*10^{-2}$	0.02

Table 3.1: Best fit values of the profile parameters: $\mathfrak{c}$ and $\frac{1}{b}$, the quadratic equation for the conic approximation: $\mathfrak{R}[\mathfrak{z}]$, the trunk parameters: $\mathfrak{e}$, $\mathfrak{C}$, and the square-root of the variance: $\sqrt{\text{variance}}$. (In the analysis, the parameters $\mathfrak{e}$, $\mathfrak{C}$ were adjusted to render the variance a minimum.) The $\sqrt{\text{variance}}$ has been normalized by dividing by the maximum trunk area to render the values comparable.

In Part 2, the bulking ratio γ was shown to be a function of both the branching ratio χ and the branching angle ω. If $d\gamma$ in (3.4) is replaced by $\frac{d\gamma}{d\chi}d\chi$ and rearranged, then

$$\frac{dA}{dz} = \left(1 - \frac{d\gamma}{d\chi}\right)\frac{da}{dz};$$

thus,

$$A[z] = \int_0^z \left(1 - \frac{d\gamma}{d\chi}\right)\frac{da[z']}{dz'}dz'. \tag{3.5a}$$

In dimensionless variables,

$$\mathfrak{U}[\mathfrak{z}] = \int_0^{\mathfrak{z}} \left(1 - \frac{d\gamma}{d\chi}\right)\frac{da[\mathfrak{z}']}{d\mathfrak{z}'}d\mathfrak{z}'. \tag{3.5b}$$

The branching ratio $d\chi$ is given by

$$d\chi = \frac{da}{A}. \tag{3.6}$$

Taking χ as its *average* over an element of distance Δz, and writing $\Delta a = \frac{da}{dz}\Delta z$. then,

$$\chi = \frac{1}{A}\frac{da}{dz}\Delta z. \tag{3.7a}$$

In dimensionless variables,

$$\chi = \frac{1}{\mathfrak{U}}\frac{da}{d\mathfrak{z}}\Delta\mathfrak{z}. \tag{3.7b}$$

For the purpose of this Part, the branching angle is set at 90° ($\omega = \frac{\pi}{2}$). As an explicit expression for γ as a function of χ is not available, an *approximate* expression was derived in the form of the third degree polynomial:

$$\gamma = 1 - \chi + (3\gamma_1 - 1)\chi^2 - (2\gamma_1 - 1)\chi^3, \tag{3.8}$$

where γ_1 is the value of γ at $\chi = 1$; in general, from (2.13),

$$\gamma_1 = \cos\left[\frac{\omega}{2}\right]. \tag{3.9}$$

If $\omega = \frac{\pi}{2}$, then $\gamma_1 = \frac{1}{\sqrt{2}}$. The coefficients of (3.8) were determined by first considering that at $\chi = 0$, $\gamma = 1$; and at $\chi = 1$, $\gamma = \gamma 1$. Then, following (2.11, 2.12), the partial derivative $(\frac{\partial\gamma}{\partial\chi})_\omega$ (i.e. ω is held constant at $\frac{\pi}{2}$) was evaluated at its limiting values; at $\chi = 0$, $(\frac{\partial\gamma}{\partial\chi})_\omega = -1$; and at $\chi = 1$, $(\frac{\partial\gamma}{\partial\chi})_\omega = 0$. The gains in both convenience and insight by using the approximation contained in (3.8) are significant.

The cross-sectional area $A[z]$ of the trunk as a function of distance from the tree top is given by (3.5a); $\frac{da}{dz}$ by (3.2). Now, $\frac{d\gamma}{d\chi}$ is just the derivative of (3.8), wherein χ can be expressed in terms of z by (3.7a). (For working purposes, I carried out this analysis using the dimensionless variables, the (b) equations.)

Equations (3.5) for area requires knowledge of χ from (3.7), which in turn requires knowledge of area. Here, the following iterative procedure was used: First, set the derivative $\frac{d\gamma}{d\chi} = 0$ (this is equivalent to setting $\gamma = 1$, no bulking-up). Then (3.5) can be integrated to yield a first approximation of area. Substitution of this expression for area into (3.7) gives $\chi[z]$. Next, substitution of $\chi[z]$ into the derivative of (3.8) yields $\frac{d\gamma}{d\chi}$ as a function of z, which, in turn, can be substituted back into the integral of (3.5) to produce a new $A[z]$. This process can be repeated as often as needed; however, convergence is fast.

3.3 Field Measurements and Analysis

Three trees of significantly different forms ($\mathfrak{k}$ values) were selected (Tab. 3.1) for presentation: juniper (*Juniperus scopulorum*), aspen (*Populus tremuloides*), douglas-fir (*Pseudotsuga menziesii*). The determination of trunk areas as functions of position along the trunk required the direct measurement of trunk circumferences. (This requires access to the crowns of suitable, mature trees - a problem for one without a "cherry-picker"). Photographs of the trees were used to establish the profiles of the trees, thus their k values as developed in Part 1. Following the iterative procedure described above, theoretical values of area $A[z]$ were calculated (Figure 3.1a-c). The *variance* between the measured and theo-

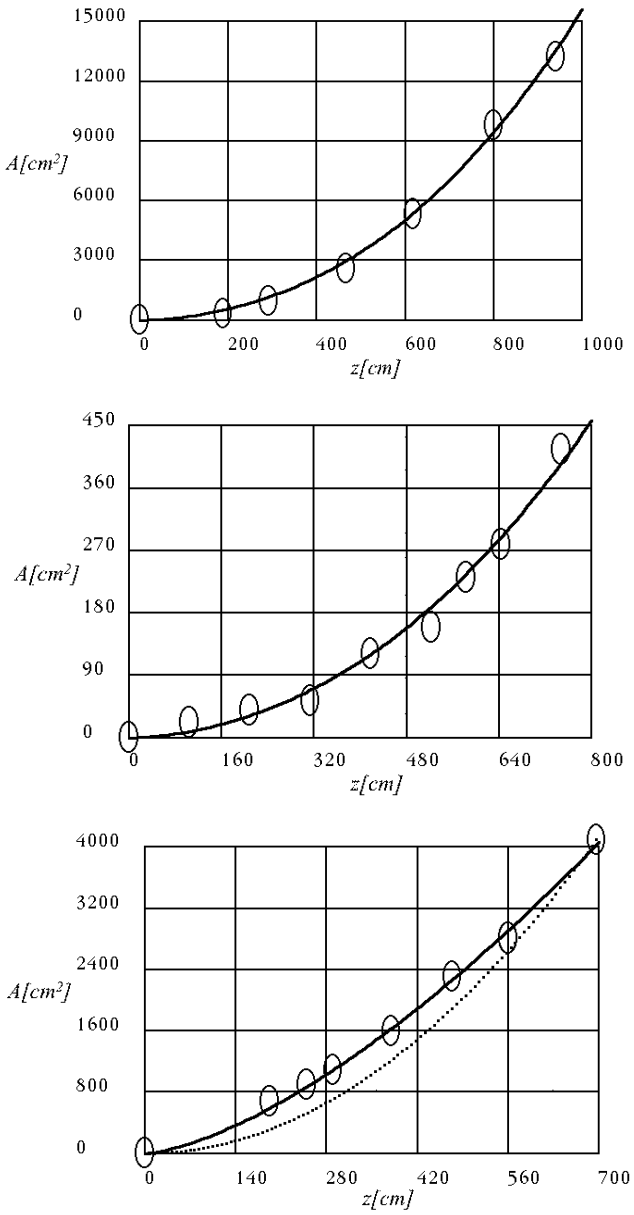

Figure 3.1: Calculated values of areas $A[z]$ and *variance* between the measured and theoretical areas for each of the three cases (a-top; b-middle; c-bottom.)

retical areas for each of the three cases was calculated.

3.4 Discussion and Summary of Part 3

In Part 3, the concepts of Parts 1 and Part 2 are tested by combining them to predict the cross-sectional area of the trunk of a tree with a single main stem and horizontal branches. No new concepts are introduced. To further simplify the analysis, conic approximations (as introduced in Part 1) are used to represent the profile $R = R[z]$.

The data is well matched by the theory as shown in the Figure 3.1 wherein the two free parameters, $\mathfrak{e}$, $\mathfrak{C}$. are adjusted to find the (unique, I believe) minimum in the variance. As in other aspects of this study, the minimum is broad with respect to the two parameters. Although the results of this Part support the concepts of Parts 1 and 2, it must be cautioned that other two parameter models (quadratic) can also be adjusted to fit the data.

The dotted curve in Figure 3.1c gives the trunk area if the trunk were a perfect cone with base near $z =$ 700cm. This curve is presented because a trunk is often modeled as a cone in estimating the volume of wood, an approximation which seems to under-estimates the volume, as would be prudent.

General Summary

The results of this study does not constitute a tree model in the manner of the pipe models of (Shinozaka et al. 1964a,b), (Valentine 1985), (Rennolls 1992), etc., but it presents theoretical considerations relevant to such whole-tree models.

The basic assumption here is that the architecture of the tree will be such as to minimize plant tissue while providing for the tree's needs. In Part 1, the overall shape of trees is considered, with an eye to the distribution of leaves (photosynthetic units); in Part 2, branching is considered, with the angle of branching of primary interest. The mode of investigation is mathematical, with the calculus of variation the central tool. The models developed are checked against field measurements. Although the agreement between theory and measurement is reasonable it falls far short of "validating" the models. Only the most obvious of predictions are tested. The possible taxonomic connections suggested by the models are barely touched upon.

Although it is this author's intention to continue the field work, there are problems in my so-doing: Access to the canopies of mature trees is difficult in most cases. Finding trees that are more-or-less undeformed by crowding, damage, or disease is often an issue; most trees in an open forest are suitable for my purposes, but obtaining telephoto images of individual trees is difficult And most challenging is finding ways to easily and cheaply measure leaf density; direct leaf counting is unduly tedious.

The theoretical results take the form of constrained minimizations. In both cases (Parts 1 and 2) the minima are shallow and broad, meaning that the tree does not pay a serious price in plant tissue (as measured by the present models) in deviating from the optimum. The author is quite aware that factors other than the ones

considered here are important in tree morphology. However, the agreement between theory and measurement is sufficiently good to suggest that the ideas presented here be considered reasonable hypotheses.

Acknowledgements

I am especially pleased to thank my wife, Loraine Yeatts, for help in all aspects of this work: she did nearly all the photography, assisted with most of the field work, and provided expertise on all botanical matters. My thanks also to Priscilla Spears (who also contributed some photos of trees), Rick Brune, and Carol English for helpful discussions. I am very much indebted to the editors of MCFNS and to the reviewers of this paper for their encouragement and further recommendations on the literature.

References

Bell, Adrian D. and Alan Bryan. 1991. Plant Form: An Illustrated Guide to Plant Morphology. Oxford. 341p.

Berninger, Frank, Lluis Coll, Petteri Vanninen, Annikki Makela, Sari Palmroth, and Eero Nikinmaa. 2005. Effects of tree size and position in pipe model ratios in Scots pine. Can. J. For. Res. 35:1294-1304.

Emerson, Robert. 1929. Photosynthesis as a function of light intensity and of temperature with different concentrations of chlorophyll. Journal of General Physiology 12(5): 623-639.

Hall, D. O. and K. K. Rao. 1999. Photosynthesis, Sixth Edition. Cambridge. 214p.

Horn, Henry S. 1971. *Trees*, Princeton. 144p.

Kantola, Anu, Harri Makinen, and Annikki Makela. 2007. Stem form and branchiness of Norway spruce as a sawn timber - Predicted by a process based model. Forest Ecology and Management 241:209-222.

Makela, Annikki. 2002. Derivation of stem taper from pipe theory in a carbon balance framework. Tree Physiology 22:891-905.

Makela, Annikki and Harry Valentine. 2006. Crown Ratio Influences Allometric Scaling in Trees. Ecology 87:2967-2972.

Mitchell, Kenneth J. 1975a. Dynamic and simulated yield of Douglas-fir. For. Sci. Monogr. 21(4):1-40.

Mitchell, Kenneth J. 1975b. Stand description and growth simulation from low-level stereo photos of tree crowns. J. For., January:12-17.

Rennolls, Keith. 1994. Pipe-model theory of stem-profile development. Forest Ecology and Management. 69:41-55.

Savage, V. M., L. P. Bentleyc; B. J. Enquistb, J. S. Sperryd, D. D. Smith, P. B. Reiche, and E. I. von Allmend. 2010. Hydraulic trade-offs and space filling enable better predictions of vascular structure and function in plants. PNAS 107(107) :22722-22727.

Shigo, Alex L. 1994. *Tree Anatomy*, Shigo and Trees, Associates. 104p.

Shinozaki, K., K. Yoda, K. Hozumi, and T. Kira (1964) A quantitative analysis of plant form: the pipe model theory. I. basic analyses. Japanese Journal of Ecology 14:97-105.

Tausch, Robin J. 2009. A Structurally Based Analytic Model for Estimation of Biomass and Fuel Loads of Woodland Trees. Natural Resource Modeling, 22(4): 463-488.

Thomas, Peter. 2000. *Trees: Their Natural History*. Cambridge. 286p.

Tiangco, Peter N. and Bruce C. Forester. 2000. Development of trunk-canopy biomass and morphology indicies from quadpolarized radar. URL: http://gisdevelopment.net/aars/acrs/2000/ts12/ts1203pf.htm

Valentine, Harry. 1985. Tree growth models:Derivations employing the pipe-model theory. J. theor. Biol. 117: 579-585.

Valentine, Harry T., Anthony R. Ludlow, and George M. Furnival. 1994. Modeling crown rise in even-aged stands of Sitka spruce or loblolly pine. Forest Ecology and Management 69:189-197.

Valentine, Harry and Annikki Makela. 2005. Bridging process-based and empirical approaches to modeling treee growth. Tree Physiology 25:769-779.

Wang, Mingliang and Kieth Rennolls. 2007. Bivariate Distribution Modeling with Tree Diameter and Height Data. Forest Science 53:16-24.

Waring, R. H., P. E. Schroeder, and R. Owen. 1982. Applications of pipe model theory to predict canopy leaf area. Can. J. For. Res. 12:556-560.

West, G. B., J. H. Brown, and B. J. Enquist. 1997. A General Model for the Origin of Allometric Scaling Laws in Biology. Science 276:122-126.